Effects of the PDO Phase on the Tropical Belt Width

BARBARA GRASSI AND GIANLUCA REDAELLI

CETEMPS/Department of Physics, University of L'Aquila, Coppito-L'Aquila, Italy

PABLO OSVALDO CANZIANI

PEPACG, Pontificia Universidad Católica Argentina, and CONICET, Buenos Aires, Argentina

GUIDO VISCONTI

CETEMPS/Department of Physics, University of L'Aquila, Coppito-L'Aquila, Italy

(Manuscript received 6 May 2011, in final form 2 November 2011)

ABSTRACT

Recent studies have shown that the tropical belt (TB) has progressively expanded since at least the late 1970s. This trend has been largely attributed to the radiative forcing due to greenhouse gas (GHG) increase and stratospheric ozone depletion, even if an influence of sea surface temperature (SST) anomalies has been also suggested. The impact of the Pacific decadal oscillation (PDO) on the TB width is investigated in this work. The study is performed by using both Atmospheric Model Intercomparison Project (AMIP) and idealized simulations, produced by the NCAR Community Atmosphere Model, version 3 (CAM3) GCM and reanalysis data [40-yr European Centre for Medium-Range Weather Forecasts (ECMWF) Re-Analysis (ERA-40), ERA-Interim, and Modern-Era Retrospective Analysis for Research and Applications (MERRA)]. Reanalyses show that a switch of the PDO from a positive to a negative phase can lead to a significant TB expansion during the equinoxes. This effect, indicating a possible PDO contribution to the widening that characterized the TB width during the last decades, is not correctly reproduced by model simulations. Deficiencies in the sensitivity of model-simulated convective processes to SST anomalies are suggested as a possible cause of the TB widening underestimation.

1. Introduction

The existence of a widening of the tropics, since at least the end of the 1970s, has been shown by a growing number of studies published in referred literature. The tropical expansion has been extensively studied in terms of tropospheric circulation and hydrology by using radiosonde data as well as dynamical data from reanalyses (Seidel and Randel 2007; Birner 2010) and outgoing longwave radiation (OLR) data from satellites (see, e.g., Hu and Fu 2007). Also, model simulations have been used to try to reproduce the observed trend and to identify related mechanisms and possible causes. Assuming an anthropogenic origin for the observed widening, possible relationships between the width of the tropical belt (TB) and global warming have been investigated by studying the effect of the direct radiative forcing, due to the perturbation by greenhouse gases (GHG), and the indirect boundary forcing, driven by sea surface temperature (SST). Lu et al. (2007) diagnosed aspects of the tropical tendency—in particular of the weakening and poleward expansion of the Hadley cell (HC)—in the Intergovernmental Panel on Climate Change (IPCC) Fourth Assessment Report (AR4) project climate change simulations, highlighting an underestimation of the latitudinal widening in model simulations when driven only by GHG increase. They suggest that factors other than the GHG-induced global warming, such as ozone depletion and/or natural climate variability, could have played a role in the observed expansion of the HC. Lu et al. (2009), based on model simulations, attributed to a large degree the widening trend that characterized the 1958–99 time period to the stratospheric cooling driven by GHG and stratospheric ozone depletion. However, when data after 2000 are taken into account, the observed

Corresponding author address: Barbara Grassi, University of L'Aquila, CETEMPS/Department of Physics, Via Vetoio, 67010 Coppito-L'Aquila, Italy.
E-mail: barbara.grassi@aquila.infn.it

DOI: 10.1175/JCLI-D-11-00244.1

widening of the HC appears to have occurred faster than simulated by climate models in response to radiative forcing (Johanson and Fu 2009). A possible contribution from the rather abrupt switch to a positive phase of the Pacific decadal oscillation (PDO), around 1976/77, in the TB width perturbation has been suggested in a previous study (Lu et al. 2009). The PDO is an SST climate variability pattern that shifts phase at least on an interdecadal time scale, usually about 20–30 yr, quantified by an index representing the leading principal component of North Pacific (poleward of 20°N) monthly SST variability.

To contribute to the understanding of PDO–atmosphere interactions, in this work we examine the sensitivity of the TB width to the PDO phase in data from reanalyses and from general circulation model (GCM) simulations.

Given that the PDO has shown from the end of the 1990s a tendency toward a much more frequent occurrence of a negative phase, the present study is devoted to gaining insights about the contribution of this tendency to the recent widening of the tropics that is not reproduced by models (see, e.g., Johanson and Fu 2009). We therefore study, season by season, the possible PDO-driven contribution to the interdecadal fluctuation of the TB width. The mechanism by which PDO SST anomalies affect the tropical tropopause (TT) is also investigated. Two main mechanisms have been proposed for the driving of the zonal-mean circulation response to global warming and for the associated HC perturbation (Lu et al. 2008). One of the suggested mechanisms results from an increase in static stability of the subtropical and midlatitude troposphere, while the other one follows from a strengthening of the midlatitude wind in the upper troposphere and lower stratosphere as a consequence of an increase in the meridional temperature gradient due to an upper-tropospheric warming in the tropics. In this work, the temperature field perturbations driven by the PDO phase, both in reanalysis and model data, are analyzed to identify differences and possible model weaknesses.

2. Data and methods

Three sets of reanalysis data are employed in the present study: 40-yr European Centre for Medium-Range Weather Forecasts (ECMWF) Re-Analysis (ERA-40) (Uppala et al. 2005) (1958–2002), ERA-Interim (Simmons et al. 2007) (1989–2010), and Modern-Era Retrospective Analysis for Research and Applications (MERRA) (Rienecker et al. 2011) (1979–2010).

Data from Atmospheric Model Intercomparison Project (AMIP) simulation, performed at the National Center for Atmospheric Research (NCAR) by using the Community Atmosphere Model, version 3.5 (CAM3.5) atmospheric model (Neale et al. 2008; Oleson et al. 2008) forced only with observed monthly SST fields (Hurrell et al. 2008), are also considered in the analysis. The simulated 1950–2006 time period has been taken into account.

Following Hu and Fu (2007) and Lu et al. (2007), the TB width is calculated as the width of the HC from horizontal winds streamfunction. To determine the poleward edges of the HC, we compute the zonal-mean mass flux streamfunction by vertically integrating the zonal-mean density-weighted meridional wind component from the top model level downward. We calculate the maximum of the absolute value of the streamfunction at 500 hPa, assuming then that the total width of the HC is given by the distance between the first latitude poleward of the maximum at which it becomes zero in each hemisphere.

Reanalysis datasets show a TB widening tendency that is particularly evident in ERA-Interim and increases after the end of 1990s (Fig. 1). This TB width behavior, which seems to result from a combination of a long-term trend of the northern HC edge poleward shift and a sizeable poleward perturbation of the southern HC edge during the late 1990s, is not reproduced by AMIP–CAM simulation. The underestimation of this TB widening shown by CAM is common to many other atmospheric-only and coupled model simulations (cf. Johanson and Fu 2009). Note also that major TB width fluctuations can be found in all the reanalysis datasets when these overlap. In other words, the observed variations in the tropical tropopause are overall consistent in the different reanalyses. ERA-40 also seems to suggest a shift in the TB width, which is coincident with the abrupt 1976/77 climate shift, even if care has to be taken when presatellite reanalysis data are considered. While partially capturing this process, the AMIP–CAM does not show as large a change.

The influence of the PDO phase on the TT is studied by considering the mean seasonal variability of the TB width. To this end, a correlation analysis is performed between seasonal values of the TB width and the PDO index provided by the Joint Institute for the Study of the Atmosphere and Ocean (JISAO; http://jisao.washington.edu/). Furthermore, a singular value decomposition (SVD) analysis is performed on the cross-covariance matrix between two-dimensional (pressure–latitude zonal-mean cross sections) meteorological fields from different datasets and the PDO index to identify modes of behavior that are strongly coupled. The significance of the SVD analysis is computed using a Monte Carlo approach, as described in Wallace et al. (1992). A multiple linear regression fit (see Agosta and Canziani 2011 and references therein; Agosta et al. 2012) is used on both reanalysis and AMIP–CAM simulation data

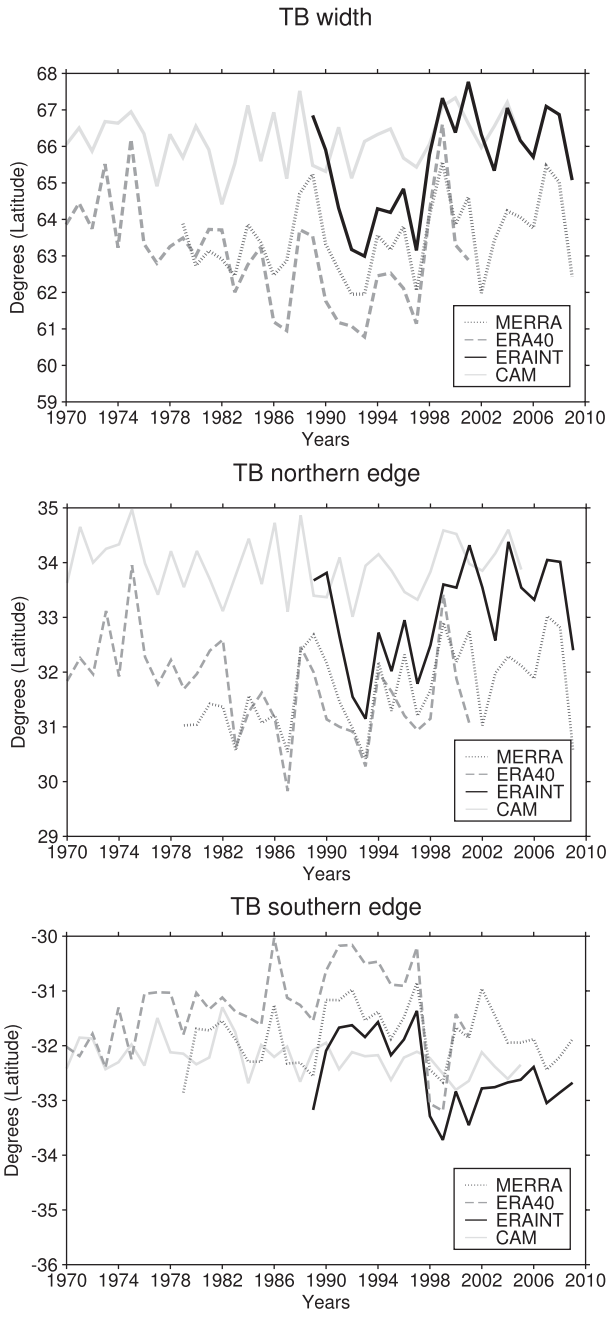

FIG. 1. Annual time series of (top) TB width and of latitudinal location of (middle) northern and (bottom) southern TB edges from reanalysis and AMIP–CAM simulation.

in order to estimate the ENSO and PDO contribution to the variability of meteorological fields. The fit takes into account the PDO and ENSO variability using the JISAO PDO index and the multivariate ENSO index (MEI; http://www.esrl.noaa.gov/psd/enso/mei/). Resulting coefficients are used to remove/minimize the ENSO or PDO contribution from the original data, resulting in what we will hereafter call ''ENSO-filtered'' and ''PDO-filtered'' fields, respectively. However, it would be more correct, because of the fact that PDO and ENSO processes are not completely independent, to speak of a minimization rather than of a total removal from the original data of the PDO or ENSO contributions. The PDO, according to Alexander (2010), may be viewed as a multiprocess phenomenon to which various mechanisms such as the Aleutian low, shifts in the North Pacific gyres, and ENSO itself, among others, contribute in different ways. Therefore, in this sense, it may be argued that the PDO is driven to a certain extent by ENSO. However, the contribution to PDO by the various processes involved is complex, scale dependent, and may even be considered random when considering regime shifts (Newman 2007). Folland et al. (2002) also used a similar linear approach to separate the Interdecadal Pacific Oscillation (IPO) (a full Pacific basin manifestation of the PDO) from ENSO signals, showing a quasi-independent influence of the two processes on the South Pacific convergence zone (SPCZ). Given these considerations, the filtering method applied here can be considered a preliminary approach to try to identify the PDO signal in the global atmospheric variability, which is affected in a very complex way by different processes not completely independent one from the other. Note that partial correlations were used in order to assess, before running the SVD analysis, the possibility of filtering of PDO and ENSO, following Canziani et al. (2008) and Agosta et al. (2012).

To reproduce the atmospheric response to oceanic conditions representative of positive and negative PDO phases, two sets of idealized ensemble simulations have been performed with the CAM3.1 model (Collins et al. 2006). The model has been used at a T42 resolution (about 2.8° × 2.8°) with 26 vertical layers in a hybrid-sigma coordinate system, ranging from the surface to 2.917 hPa, with a vertical resolution varying in the stratosphere from 1.1 to 3–4 km in the upper levels. While the standard dataset provided with the model is used for sea ice and ozone, SST boundary conditions are calculated from the National Oceanic and Atmospheric Administration (NOAA) extended reconstructed SST dataset version 3 (ERSST.v3) (Smith et al. 2008), spanning the negative PDO phase period after 2000 and showing, compared to other SST datasets, a much stronger projection onto the Pacific pattern (Pegion and Kumar 2010).

Using the JISAO PDO index, we identified a characteristic pattern of the SST PDO anomalies from ERSST.v3 data by compositing years characterized by positive/negative PDO index values (Fig. 2) over the 1948–2008 time frame. Two sets of simulations, hereafter referred as ''PDO_POS'' and ''PDO_NEG'' cases, have been then performed by specifying SST boundary

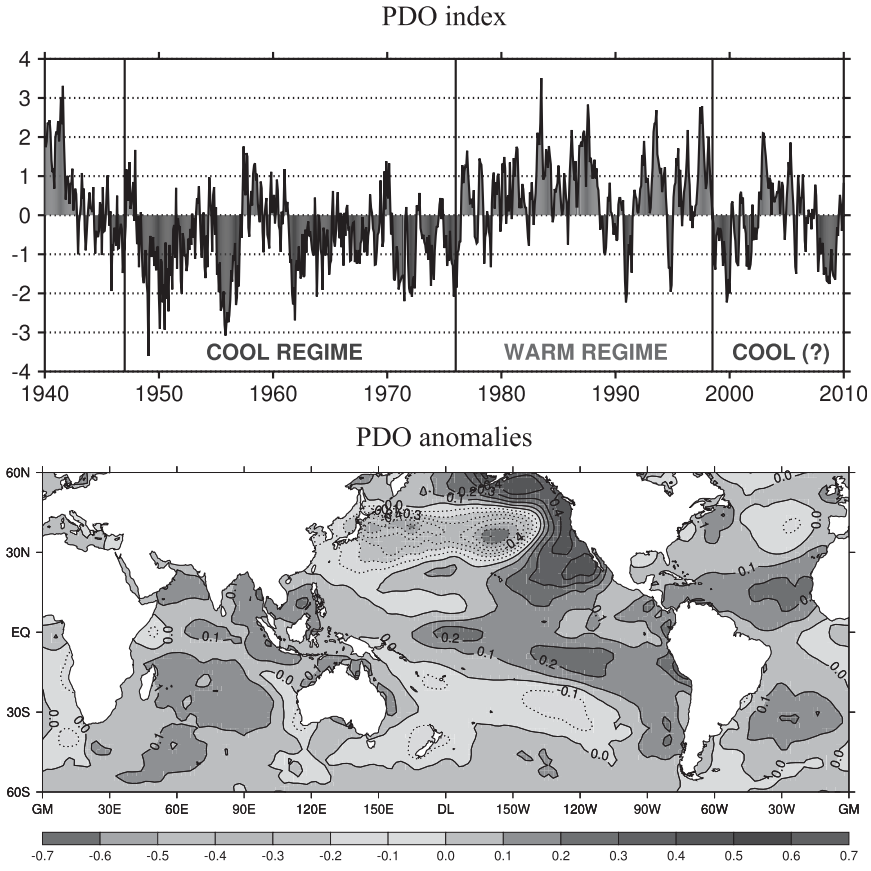

FIG. 2. (top) Monthly PDO index values since 1940 and (bottom) PDO SST anomaly pattern used in the study. See text for discussion.

conditions obtained by considering monthly varying SST climatological values plus or minus, respectively, the calculated PDO anomalies. The simulated cases differ only in the monthly SST fields used for the boundary conditions that are given as an annual cycle repeated each year. Following the approach used in previous studies (Grassi et al. 2008) (i.e., considering the same annual cycle of the boundary conditions), we run the model for 10 consecutive years, producing an ensemble of 10 yearly realizations to generate a statistical base for analysis. We study the seasonal changes of TB width in one set of simulations with respect to the other to evidence the effects of the PDO phase shift. The significance of the difference in means between the two ensemble experiments is assessed using a Student's *t* test.

3. Results

Figures 3a,b show results of the correlation analysis performed between seasonal values of zonal-mean TB widths from reanalyses and the (inverted sign) PDO index, considering both the "unfiltered" and the ENSO-filtered fields. Note that the sign of the PDO index is inverted in the analysis so that a positive value of the correlation coefficient reflects a TB widening corresponding to a decrease in PDO index. These results are consistent with the SPCZ analysis by Folland et al. (2002) where they observed, particularly in the western South Pacific, its meridional displacement—equatorward during the warm IPO and poleward during the cold IPO.

The analysis performed on the unfiltered fields shows an overall direct correlation. However, when the direct ENSO contribution is "filtered out," this results in a correlation value decrease, which is strongest during boreal winter, further supporting the use of regression analysis applied to minimize the direct ENSO signal on the TB width, and highlights an equinox PDO contribution to the TB width characterized by a statistically significant expansion during boreal spring [March–May (MAM)] and autumn [September–November (SON)]. The same correlation analysis has been also performed between seasonal zonal-mean TB width, calculated from AMIP–CAM simulation, and the (inverted sign) PDO index (Figs. 3c,d). The seasonality of the simulated

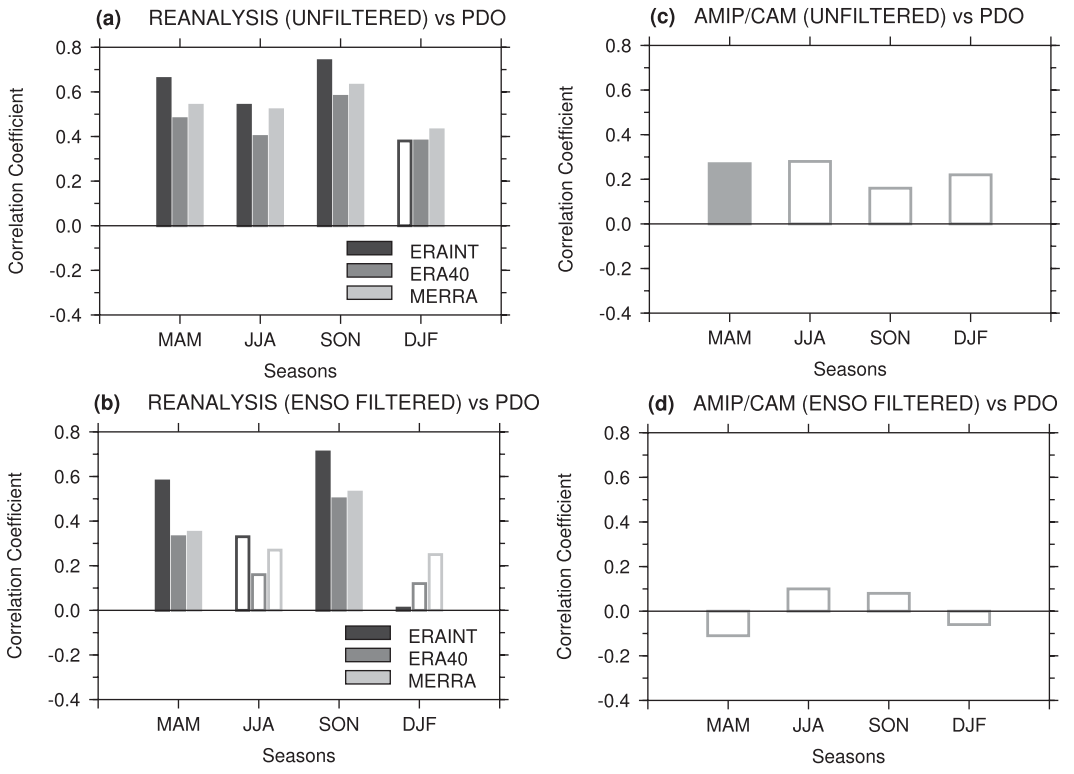

FIG. 3. (left) Correlation between zonal-mean TB width and (inverted sign) PDO index, performed both on (a) unfiltered and (b) ENSO-filtered reanalysis data (see text for definitions). (right) As in (left) but for AMIP simulation data. Shadings indicate statistical significance higher than 95%.

effect on the TB width appears to significantly differ from the effect found in reanalysis data. Also, these results are not statistically significant at the 95% level, with the only exception being the analysis for MAM performed on unfiltered field. On the contrary, the correlation analysis performed between seasonal values of PDO-filtered zonal-mean TB widths calculated from AMIP–CAM simulation data (Fig. 4b) and the (inverted sign) ENSO index shows statistically significant correlation values indicating, for all seasons, a general widening of the TB width linked to La Niña events, with highest correlation values during boreal winter and spring and lowest during summer, which is in agreement with the known seasonal impacts of ENSO events. The same correlation study performed on reanalysis data (Fig. 4a) highlights, as expected, highest correlation values during winter and, at the same time, a tendency toward lower correlation coefficient values as well as lower statistical significance during the boreal autumn when the correlation with PDO has a maximum. Note that the results are consistent for all three sets of reanalyses considered.

The discrepancy between results from reanalysis and GCM data and, in particular, the absence of a statistically significant signal in the correlation between AMIP–CAM TB width and PDO index seems to suggest a model weakness in reproducing the atmospheric variability driven by SST PDO anomalies. To investigate this hypothesis we analyze the atmospheric response in idealized GCM simulations where SST forcing only for either a PDO positive or negative mode at a time is specified (PDO_POS and PDO_NEG cases, respectively). The model response to different PDO phases is studied in terms of seasonal ensemble-mean TB width perturbation (Fig. 5a) and compared to composite differences of the TB width, calculated between years with negative and positive PDO index values both for AMIP–CAM simulation and reanalysis data (Figs. 5b,c). Composite differences confirm results from the correlation analyses, showing again an equinox PDO contribution to the TB width in reanalyses for all the datasets considered here but no significant signal in the model simulations. Results from reanalyses provide also indications about the intensity of the averaged PDO-driven widening, which, during MAM and SON, is of about 1° in latitude with maximum values for ERA-Interim of about 1.6° and minimum values for MERRA during MAM of about 0.5°. Results from idealized CAM runs confirm the absence of the PDO signal in model simulations, showing a seasonally

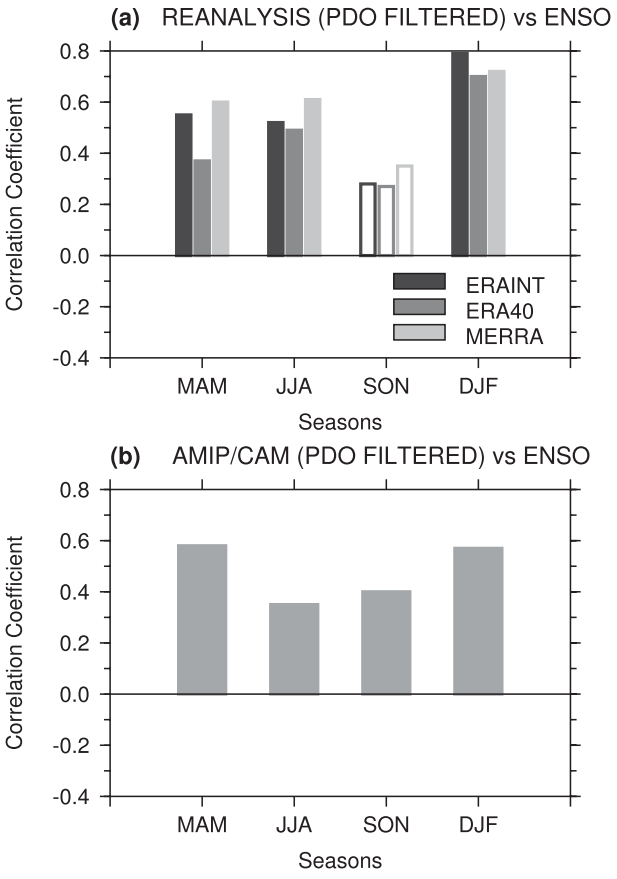

FIG. 4. Correlation between zonal-mean TB width and (inverted sign) ENSO index, performed on PDO-filtered (a) reanalysis data and (b) AMIP–CAM simulation data (see text for details). Shadings indicate statistical significance higher than 95%.

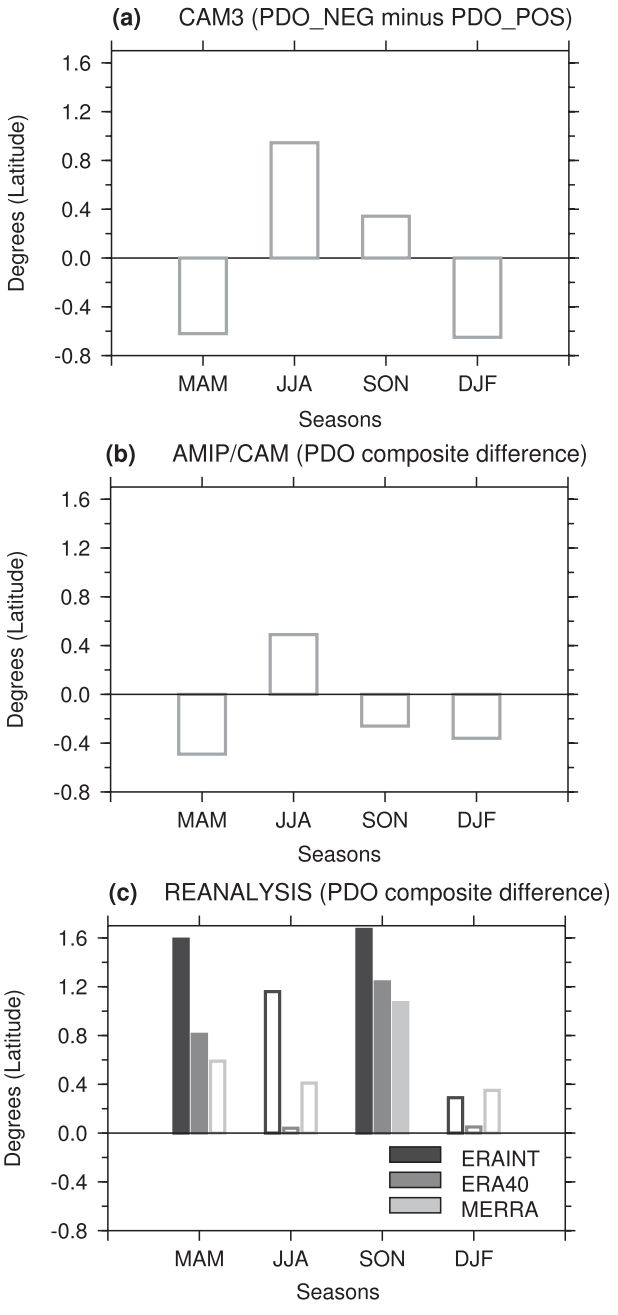

FIG. 5. (a) Differences of ensemble-mean TB width calculated between PDO_NEG- and PDO_POS-simulated cases. (b),(c) Composite difference of zonal-mean TB width (°), calculated between years with negative and positive PDO index values, from ENSO-filtered AMIP–CAM and reanalysis data, respectively. Shadings indicate statistical significance higher than 95%.

varying TB width perturbation that is not statistically significant.

To further study the described discrepancies, we examine the heterogeneous correlation maps (generally defined as the vectors of correlation values between the expansion coefficient of one field expansion mode and the grid point values of the other field we want to correlate to it) resulting from an SVD analysis applied to the time series of the two-dimensional (pressure–latitude) cross section of temperature and meridional (pole to equator) temperature gradient ENSO-filtered fields from ERA-Interim and AMIP–CAM simulation data and the time series of the (inverted sign) PDO index for MAM (Fig. 6) and SON (Fig. 7). Given that the PDO index is a monodimensional time series, the heterogeneous maps directly show the correlation coefficient between the time series of the field anomalies at each grid point and the PDO index. Differences between model and reanalysis arise both in the extratropical and tropical region. In particular, in the extratropics, the SVD map for MAM, calculated from ERA-Interim data, reveals a significant positive signal in the troposphere around 40° of latitude, which is not shown by model simulation (Figs. 6a,c), while the SVD map for SON from simulation shows a positive signal in the southern region not present in results from

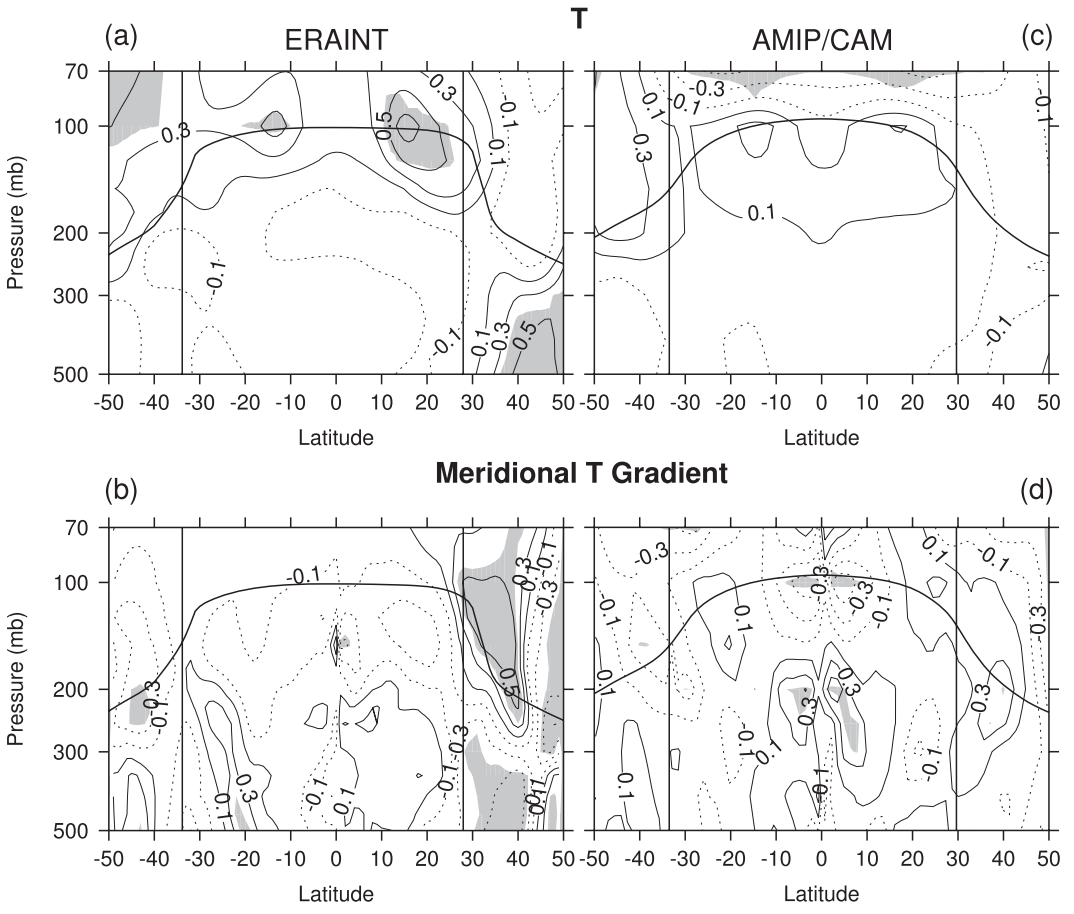

FIG. 6. SVD maps, for MAM, calculated between the ENSO-filtered two-dimensional time series of temperature and equator-to-pole temperature gradient, from (a),(b) ERA-Interim data and (c),(d) AMIP–CAM simulation data, and the inverted PDO index time series. Average lapse-rate tropopause height and tropical belt edges, as calculated by ERA-Interim data and simulated by CAM, are also shown. Shadings indicate statistical significance higher than 95%.

reanalyses (Figs. 7a,c). These differences, probably related to large-scale circulation response, can also be found when ensemble-mean differences between idealized simulation cases (not shown) are considered. More interesting, from our point of view, appears to be the differences affecting the tropical region. The results for ERA-Interim show a general warming signal, appearing at the tropical tropopause level, which has two maxima—almost symmetric with respect to the equator. The same feature was found in the SVD maps calculated from ERA-40 and MERRA (not shown here). Model results, while reproducing the positive correlation near the tropical tropopause, underestimate this signal, showing correlation values that are lower and not statistically significant. The described warming on the ERA-Interim temperature correlation maps at the tropopause level leads to the generation of a positive meridional temperature gradient at the northern and southern poleward flank of the tropopause slope for MAM and SON, respectively (Figs. 6b and 7b). In agreement with the mechanism suggested by Lu et al. (2008), the increase of the meridional temperature gradient near the tropopause level can lead to the strengthening of the midlatitude winds at the upper tropopause and lower stratosphere. This can in turn produce a poleward shift of the HC edge through the increase of the eastward propagation of midlatitude eddies and the subsequent poleward displacement of the subtropical wave-breaking region, resulting in a widening of the TB.

We suppose that the tropopause warming could be driven by a perturbation of convective process activation. In fact, tropical upwelling has been found to be anticorrelated with tropopause temperature (e.g., Randel et al. 2006 and references therein) and systematic decrease in deep convection can potentially lead to a tropopause warming. Also, previous studies have suggested that GCMs often lack variability in the level of convective activity in the tropics (e.g., Willett et al. 2008 and references therein). Based on these considerations, we suggest

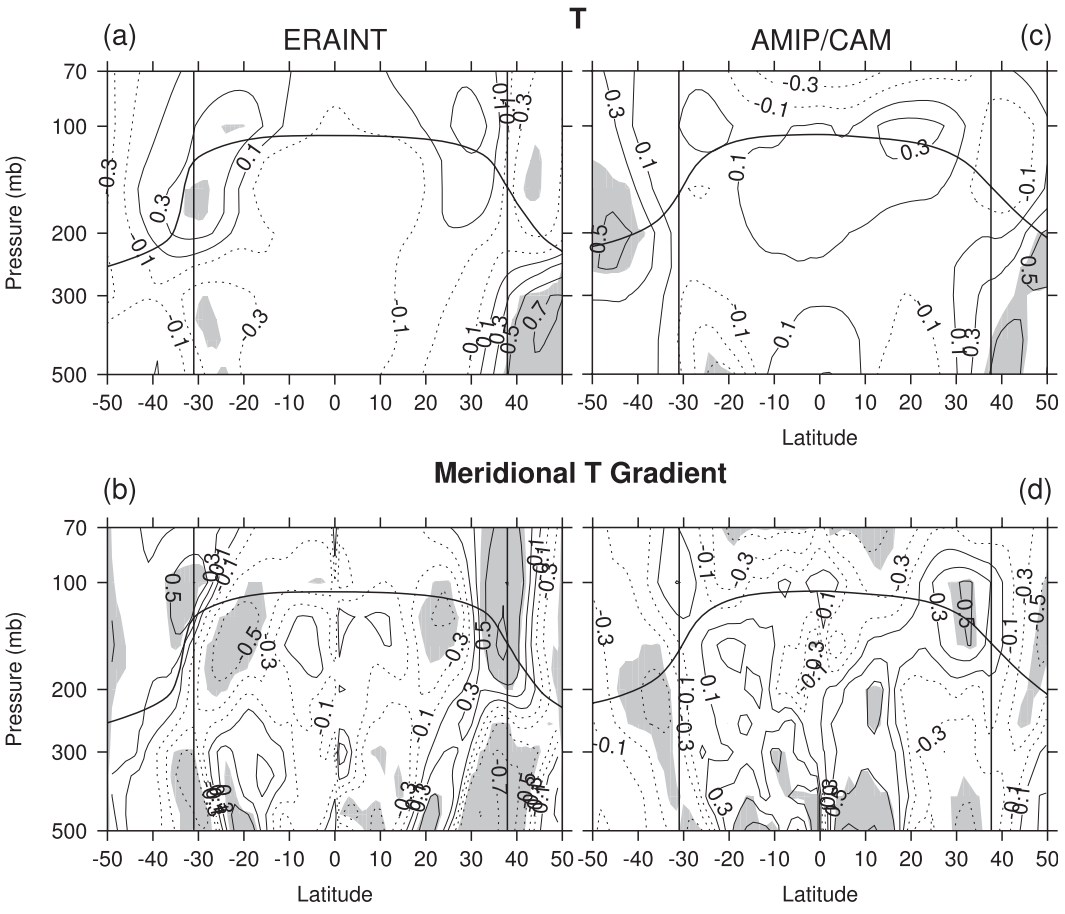

FIG. 7. As in Fig. 6, but for SON.

that an incorrect estimation of convective process perturbation could lead to the lack of the TB width signal in model simulations. Additional research and analyses would be necessary to further support this hypothesis.

4. Conclusions

Three sets of reanalyses have been used to study possible relationships between TB width and PDO decadal phase variability. Results evidence an equinox TB tendency to be wider when PDO index shifts from positive to negative values as a consequence of perturbations in the temperature meridional gradient at the edges of the TB. This effect could have contributed to the TB widening observed during last decades, when PDO shows a tendency toward more frequent occurrences of the negative phase. The study also suggests a deficiency in the model-simulated temperature tropopause response to the PDO variability that is probably related to a weak response to PDO SST anomalies in terms of convective process activation. We speculate that this weakness could possibly lead to the general model underestimation, highlighted by previous studies, of the TB widening observed at the end of 1990s.

Acknowledgments. NOAA/ERSST.v3 and MEI data are provided by NOAA/OAR/ESRL (http://www.esrl.noaa.gov/). The PDO index is provided by JISAO (http://jisao.washington.edu/). The authors acknowledge the ANPCyT PICT 2007 ICES-IDAC 01888 Grant, UCA for partially supporting the research; NCAR for making the CAM3.5 runs available (http://gmao.gsfc.nasa.gov/); and the Global Modeling and Assimilation Office (GMAO) and the GES DISC for the dissemination of MERRA. The authors also thank three anonymous reviewers for their valuable comments and suggestions.

REFERENCES

Agosta, E. A., and P. O. Canziani, 2011: Austral spring stratospheric and tropospheric circulation interannual variability. *J. Climate,* **24,** 2629–2647.

——, ——, and M. A. Cavagnaro, 2012: Regional climate variability impacts on the annual grape yield in Mendoza, Argentina. *J. Appl. Meteor. Climatol.,* in press.

Alexander, M., 2010: Extratropical air-sea interaction, sea surface temperature variability, and the Pacific decadal oscillation. *Climate Dynamics: Why Does Climate Vary? Geophys. Monogr.,* Vol. 189, Amer. Geophys. Union, 123–148.

Birner, T., 2010: Recent widening of the tropical belt from global tropopause statistics: Sensitivities. *J. Geophys. Res.,* **115,** D23109, doi:10.1029/2010JD014664.

Canziani, P. O., F. E. Malanca, and E. A. Agosta, 2008: Ozone and upper troposphere/lower stratosphere variability and change at southern midlatitudes 1980–2000: Decadal variations. *J. Geophys. Res.,* **113,** D20101, doi:10.1029/2007JD009303.

Collins, W. D., and Coauthors, 2006: The formulation and atmospheric simulation of the Community Atmosphere Model Version 3 (CAM3). *J. Climate,* **19,** 2144–2161.

Folland, C. K., J. A. Renwick, M. J. Salinger, and A. B. Mullan, 2002: Relative influences of the Interdecadal Pacific Oscillation and ENSO on the South Pacific convergence zone. *Geophys. Res. Lett.,* **29,** 1643, doi:10.1029/2001GL014201.

Grassi, B., G. Redaelli, and G. Visconti, 2008: Tropical SST preconditioning of the SH polar vortex during winter 2002. *J. Climate,* **21,** 5295–5303.

Hu, Y., and Q. Fu, 2007: Observed poleward expansion of the Hadley circulation since 1979. *Atmos. Chem. Phys.,* **7,** 5229–5236.

Hurrell, J. W., J. J. Hack, D. Shea, J. M. Caron, and J. Rosinski, 2008: A new sea surface temperature and sea ice boundary dataset for the Community Atmosphere Model. *J. Climate,* **21,** 5145–5153.

Johanson, C. M., and Q. Fu, 2009: Antarctic atmospheric temperature trend patterns from satellite observations. *Geophys. Res. Lett.,* **34,** L12703, doi:10.1029/2006GL029108.

Lu, J., G. A. Vecchi, and T. Reichler, 2007: Expansion of the Hadley cell under global warming. *Geophys. Res. Lett.,* **34,** L06805, doi:10.1029/2006GL028443.

——, G. Chen, and D. M. W. Frierson, 2008: Response of the zonal mean atmospheric circulation to El Niño versus global warming. *J. Climate,* **21,** 5835–5851.

——, C. Deser, and T. Reichler, 2009: Cause of the widening of the tropical belt since 1958. *Geophys. Res. Lett.,* **36,** L03803, doi:10.1029/2008GL036076.

Neale, R. B., J. H. Richter, and M. Jochum, 2008: The impact of convection on ENSO: From a delayed oscillator to a series of events. *J. Climate,* **21,** 5904–5924.

Newman, M., 2007: Interannual to decadal predictability of tropical and North Pacific sea surface temperatures. *J. Climate,* **20,** 2333–2356.

Oleson, K. W., and Coauthors, 2008: Improvements to the Community Land Model and their impact on the hydrological cycle. *J. Geophys. Res.,* **113,** G01021, doi:10.1029/2007JG000563.

Pegion, P. J., and A. Kumar, 2010: Multimodel estimates of atmospheric response to modes of SST variability and implications for droughts. *J. Climate,* **23,** 4327–4341.

Randel, W. J., F. Wu, H. Vömel, G. E. Nedoluha, and P. Forster, 2006: Decreases in stratospheric water vapor after 2001: Links to changes in the tropical tropopause and the Brewer-Dobson circulation. *J. Geophys. Res.,* **111,** D12312, doi:10.1029/2005JD006744.

Rienecker, M. M., and Coauthors, 2011: MERRA: NASA's Modern-Era Retrospective Analysis for Research and Applications. *J. Climate,* **24,** 3624–3648.

Seidel, D. J., and W. J. Randel, 2007: Recent widening of the tropical belt: Evidence from tropopause observations. *J. Geophys. Res.,* **112,** D20113, doi:10.1029/2007JD008861.

Simmons, A., S. Uppala, D. Dee, and S. Kobayashi, 2007: ERA-Interim: New ECMWF reanalysis products from 1989 onwards. *ECMWF Newsletter,* No. 110, ECMWF, Reading, United Kingdom, 25–35.

Smith, T. M., R. W. Reynolds, T. C. Peterson, and J. Lawrimore, 2008: Improvements to NOAA's historical merged land–ocean surface temperature analysis (1880–2006). *J. Climate,* **21,** 2283–2296.

Uppala, S. M., and Coauthors, 2005: The ERA-40 Re-Analysis. *Quart. J. Roy. Meteor. Soc.,* **131,** 2961–3012.

Wallace, J. M., C. Smith, and C. S. Bretherton, 1992: Singular value decomposition of wintertime sea surface temperature and 500-mb height anomalies. *J. Climate,* **5,** 561–576.

Willett, M. R., P. Bechtold, D. L. Williamson, J. C. Petch, S. F. Milton, and S. J. Woolnough, 2008: Modelling suppressed and active convection: Comparisons between three global atmospheric models. *Quart. J. Roy. Meteor. Soc.,* **134,** 1881–1896.